Mechanistic study to investigate the effects of different gas injection scenarios on the rate of asphaltene deposition: An experimental approach

Hossein Dashti [a,b,1], *Peyman Zanganeh* [c,1], *Shahin Kord* [d], *Shahab Ayatollahi* [e,*], *Amirpiran Amiri* [f]

[a] School of Chemical Engineering, The University of Queensland, Brisbane, Australia
[b] Centre for Coal Seam Gas, The University of Queensland, Brisbane, Australia
[c] Department of Chemical Engineering, School of Chemical Engineering, Shahid Bahonar University of Kerman, Kerman, Iran
[d] Ahwaz Faculty of Petroleum, Petroleum University of Technology (PUT), Ahwaz, Iran
[e] Sharif Upstream Petroleum Research Institute, Department of Chemical and Petroleum Engineering, Sharif University of Technology, Tehran, Iran
[f] European Bioenergy Research Institute (EBRI), School of Engineering and Applied Science, Aston University, Birmingham, B4 7ET, United Kingdom

[1] The first two authors contributed equally to this work.
[*] Corresponding author, Email: shahab@sharif.ir, Tel/Fax: +98 21 66166411

Abstract

Asphaltene deposition during enhanced oil recovery (EOR) processes is one of the most problematic challenges in the petroleum industry, potentially resulting in flow blockage. Our understanding of the deposition mechanism with emphasis on the rate of the asphaltene deposition is still in its infancy and must be developed through a range of experiments and modelling studies. This study aims to investigate the rate of asphaltene deposition through a visual study under different gas injection scenarios. To visualise the asphaltene deposition, a high-pressure setup was designed and constructed, which enables us to record high-quality images of the deposition process over time. Present research compares the effects of nitrogen (N_2), carbon dioxide (CO_2) and methane (CH_4) on the rate of asphaltene deposition at different pressures. The experimental results in the absence of gas injection revealed that the rate of asphaltene deposition increases at higher pressures. The results showed that the rate of asphaltene deposition in the case of CO_2 injection is 1.2 times faster than CH_4 injection at 100 bar pressure. However, N_2 injection has less effect on the deposition rate. Finally, it has been concluded that the injection of CO_2 leads to more asphaltene deposition in comparison with CH_4 and N_2. Moreover, the experimental results confirmed that gas injection affects the mechanism of asphaltene flocculation and leads to the formation of bigger

flocculated asphaltene particles. The findings of this study can help for a better understanding of the mechanism of the asphaltene deposition during different gas-EOR processes.

Keywords: Enhanced oil recovery, asphaltene deposition rate, CO_2 injection, gas injection

1. Introduction

Asphaltenes are heavy crude oil fractions that are not soluble in light hydrocarbon solvents (typically n-pentane or n-heptane) but could be dissolved in light aromatic hydrocarbons (typically toluene) [1, 2]. Asphaltenes are the most polar components and have the highest molecular weight among crude oil fractions, exhibiting both aliphatic and aromatic structures [3-6]. Asphaltene particles tend to aggregate and produce more massive particles [7]. The complex physical and chemical properties of asphaltenes remain a challenge for the research community [8, 9]. Changes in pressure, temperature or composition cause the resin layer to shrink followed by asphaltene precipitation [10-13]. The reversibility or irreversibility of the asphaltene precipitation is not fully understood in the literature, and it is likely to be related to the complex structure of the asphaltene particles [7, 14, 15].

In order to establish consistent terminology, it is necessary to clarify the application of different terms. The terms “aggregation” and “flocculation” have been used to refer to the formation of the clusters of asphaltene particles in the crude oil which will result in increasing the size of the small asphaltene particles from nanometer into micrometre length scale [16]. The term “precipitation” is defined in its broadest sense to refer to the whole process of asphaltenes flocculation or aggregation from the crude oil fluid. Finally, “deposition” refers to the settling of the aggregated or flocculated asphaltene particles onto the solid surface which is mostly investigated in this work.

Asphaltene deposition in wellbores and pipelines is a technical and operation concern at various stages of oil production and processing. This problematic phenomenon has not been well understood yet mainly because of complex physicochemical properties and phase behaviour. In particular, there is a critical gap in understanding the conditions that lead to asphaltene instability [17]. Such insight into the problem physics guides engineers and operators to design and implement appropriate strategies toward an asphaltene-free operation. Asphaltene deposition can occur in the first stage of oil production or during enhanced oil recovery (EOR) [18]. Asphaltene

deposition in oil reservoirs can lower its permeability, change rock wettability from water-wet to oil-wet, and increase hydrocarbon viscosity. All of these negative impacts lead to an ongoing decline in oil production rate [19, 20]. Numerous research has shown that the tendency of asphaltene particles to deposit is strongly related to the complex structure of asphaltenes [19, 21-23]. The lost production due to asphaltene deposition is estimated to be approximately $1,200,000 per day [24]. Accordingly, asphaltene deposition can be avoided/minimised by manipulating the structure via the treatment or prevention methods [25]. The treatment approaches, however, are expensive causing process economic concerns. The possible solution for the problem of the asphaltene deposition in the oil reservoirs compared with the expensive treatments methods to remove the asphaltenes can be using inhibitors [26-29] or control the operation conditions [22, 23, 30-32]. Fig. 1 presents a schematic of the problem of asphaltene deposition with possible solutions. EOR methods are the most common approaches after primary and secondary oil production [33-37]. A growing body of literature recognises the importance of EOR processes and enhancing the effectiveness of these methods [38-44]. Carbon dioxide (CO_2), nitrogen (N_2) and methane (CH_4) flooding are commonly considered as EOR methods. Asphaltene deposition during EOR processes is one of the challenges facing the oil industry. Asphaltene deposition during CO_2 flooding in oil reservoirs has been extensively studied [21-23, 31, 32, 45-48]. However, few studies have been conducted examining the influence of N_2 and CH_4 flooding on the amount of asphaltene deposition [23, 49-53].

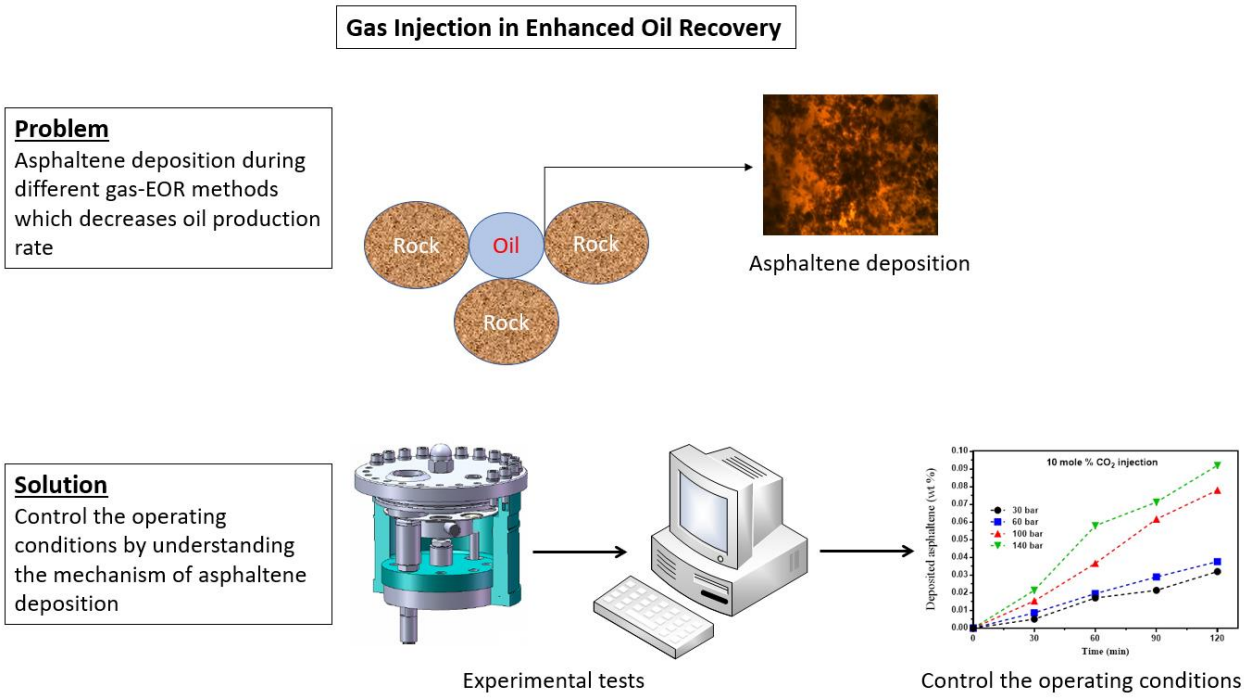

Fig. 1. Schematic of the problem of asphaltene deposition in the oil reservoirs.

The kinetics of asphaltene deposition is an area of intense debate in the research community. Although extensive research has been conducted on asphaltene aggregation kinetics and thermodynamic stability, few studies have focused on the rate of asphaltene deposition. Previous reports indicate that the process of asphaltene deposition near the wellbore region primarily depends on the rate of the process [54]. The slow kinetics of asphaltene deposition is an obstacle to understanding asphaltene behaviour [55-58]. It is reported that the kinetics of asphaltene precipitation near the onset of instability is very slow. A study by Jamialahmadi et al. (2009) investigated the rate of asphaltene deposition from crude oil [59]. These researchers observed that the oil velocity, surface and bulk temperature, and the concentration of the flocculated asphaltene are the critical parameters with a dominant influence on the rate of asphaltene deposition. The deposition rate has been observed to increase due to increases in flocculated asphaltene concentration and surface temperature. Furthermore, as the oil velocity increases, the deposition rate decreases. The same observations were reported by Soulgani et al. (2011) [60], Salimi et al. (2013) [61], Arsalan et al. (2014) [54] and Haghshenasfard and Hooman (2015) [62]. Recent work by Favero et al. (2016) studied the rate of asphaltene deposition as a function of fluid flow rate [63]. These researchers concluded that the asphaltene deposition rate could increase with the

concentration of unstable asphaltenes. The same experimental observation has been reported by Ghahfarokhi et al. (2017) [64]. Taken together; these studies clearly show that a proper understanding of the mechanism of asphaltene deposition is critical for the inhibition and/or treatment of this issue in the oil industry.

To date, there have been no controlled studies which investigated the rate of the asphaltene deposition in different EOR methods. The unsteady state analysis on the behavior of the asphaltene particles in the presence of different gasses can generate a fresh insight into the prediction and controlling asphaltene deposition phenomenon in the potential oil reservoirs. The present work attempts to study the kinetics of asphaltene deposition rate at different operating pressures under various gas injection scenarios. A tentative analysis is presented to compare the deposition rate under different gas injection conditions using a visual high-pressure experimental apparatus. The advantage of the current study is the evaluation of the asphaltene deposition rate using a visual investigation which lays the groundwork for future research into asphaltene deposition. On the other hand, the limitation on the analysis of the visual observation was a challenge in this study which has been appropriately addressed to prove the effectiveness of the proposed approach in the experiments.

The first part of this paper will present the experimental apparatus and the procedure. Then, in the results and discussion section two main issues will be addressed; the effects of the different gas injection scenarios on the asphaltene deposition rate, and analysis on the effects of the gas injection on the asphaltene flocculation to explain the possible reasons behind the results of the experimental tests.

2. Experiments

2.1. Experimental Apparatus

The high-pressure experimental apparatus was constructed and developed to visually investigate the rate of asphaltene deposition (Fig. 2). The experimental apparatus consists of a high-pressure cell with a rotating metal disc which was horizontally placed in the cell as can be seen in Fig. 3 [21-23, 64]. Nine different types of glass substrates placed on the rotating disc to investigate the process of the asphaltene deposition on the rock surface and collect the deposited asphaltene particles during the experimental tests. The substrate plates have been used in order to mimic the

sandstone in the oil reservoirs. A microscope (KRÜSS, MBL2000) with a potential optical resolution up to 480X was used on the top of the high-pressure cell to visualise the process of asphaltene deposition. A charge-coupled device (CCD) camera (IDS, UI-1485LE-C5 HQ, 5.7 megapixels) was used on the microscope to capture the high-resolution pictures from the deposited asphaltenes on the substrates. A magnetic device was installed in the cell in order to adjust each substrate in front of the microscope. The dark solution is placed on the substrate in the gap between the light source and the microscope. More details of the experimental apparatus are reported elsewhere [21-23, 64-66].

Different mole percentages of gases (N_2, CO_2 and CH_4) were injected into the cell. The process of asphaltene deposition was detected via a high-resolution microscope. Image processing software was used to determine the amount of deposited asphaltene and its size distribution under different conditions [21-23, 64-66].

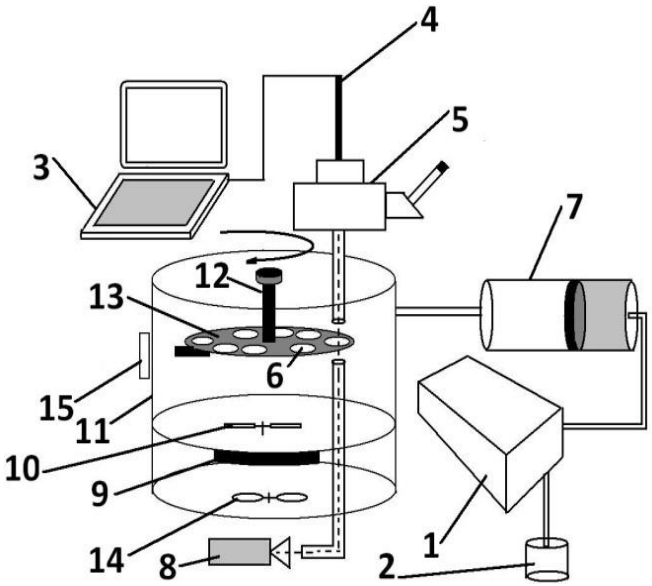

Fig. 2. Sketch of the high-pressure experimental apparatus [22]: (1) peristaltic pump, (2) distilled water reservoir, (3) computer, (4) CCD camera, (5) microscope, (6) sight glass, (7) piston-cylinder, (8) cold light source, (9) heater, (10) magnetic mixer, (11) high-pressure cell, (12) rotator, (13) metal disc, (14) fan, (15) magnetic device.

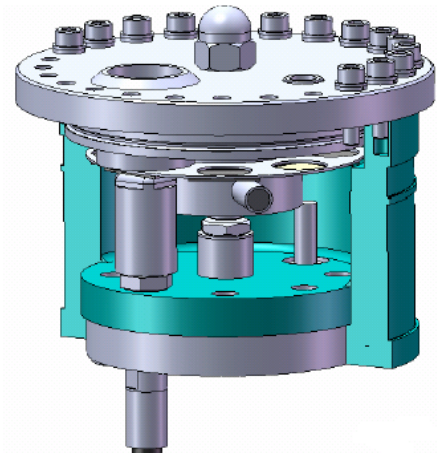

Fig 3. Schematic of the high-pressure cell to study the rate of the asphaltene deposition visually.

2.2. Experimental Procedure

A series of experiments were performed to study the asphaltene deposition rate using the following procedure: Firstly, asphaltene sample was extracted based on the method described by ASTM-D86 [67]. Synthetic oil was then prepared by mixing toluene (C_7H_8) and normal heptane (n-C_7) (Merck, high-performance liquid chromatography grade). The mixture was mixed for 1 hour using a magnetic stirrer and then used as synthetic oil. It is worth stating that the synthetic oil mixture is stable at the atmospheric pressure and its bubble point is about 0.8 bar at 90 °C. The saturate, aromatic, resin and asphaltene analysis of the crude which asphaltene extracted from that is reported in Table 1, and the synthetic oil composition is listed in Table 2. Furthermore, the results of the elemental analysis on the asphaltene type used in this study reported by Sayyad Amin et al., (2011) is presented in Table 3 [68]. They performed the elemental analysis using CHNSO analyzer to measure the mass ratio of carbon (C), hydrogen (H), sulphur (S), oxygen (O), vanadium (V) and nickel (Ni).

The thermodynamic behaviour of reservoir fluid is the primary and essential step in reservoir simulation, where a proper model should be validated and matched against the laboratory pressure, volume and temperature (PVT) data. The reservoir fluid characterisation including the tuning of the equation of state parameters using the same crude sample in this study was modelled and validated to achieve a more accurate understanding of the reservoir fluid [69].

Table 1.
Saturate, aromatic, resin, and asphaltene analysis of the field sample [23].

Test name	Saturates	Aromatics	Resins	Asphaltene
wt %	38.74	50.59	6.17	4.25

Table 2.
Synthetic oil composition used in this study [22, 23].

Components	C_7H_8	n-C_7	Asphaltene	Total
mol %	75	23	2	100

Table 3.
The elemental analysis of the asphaltene type used in this study [68].

Elements	C	H	N	S	O	Ni (ppm)	V (ppm)	Formula
wt %	74.56	6.74	0.85	6.84	10.99	0.626	0.219	$C_{102}H_{110}O_{11}N_1S_3$

The following procedure was applied to all experiments [23]:

1- Initially, the solution of the synthetic oil was injected into the cell. Then, the temperature was increased in several steps to setpoint value of 90°C at atmospheric pressure.

2- The cell was pressurised slowly to 140 bar using the high-pressure liquid chromatography pump (at constant temperature).

3- The solution was allowed to deposit asphaltene particles on the substrates. Images were taken from the glass surfaces through the microscope at equal time steps to measure the amount of deposited asphaltene. After approximately 2 hours, no more deposition was observed on the horizontal glass surfaces indicating that the equilibrium had been reached. It, therefore, was the time to proceed to the next step.

4- The pressure was decreased to 100 bar at constant temperature of 90°C. Then the solution was again stirred to remove all of the deposited asphaltene particles from the glass surfaces. Accordingly, the asphaltene deposited on the glass plates was viewed, and images were captured at the new pressure as well.

5- Previous step (4) was repeated at 60 and 30 bar pressures.

6- The amount of asphaltene deposited at each pressure and time step was estimated using the image processing software to evaluate the rate of deposition. The high-resolution images were

captured by the microscope and then analysed to evaluate the deposited asphaltene particles diameter at high pressure and temperature (real thermodynamic condition).

The deposited asphaltene particle diameter was estimated by SigmaScan Pro 5^{TM} software based on the area and darkness of each particle. At the first step, the software should be calibrated and then it could measure the size and diameter of each particle. More details of the calibration method have been described in the **Supplementary Material**. After the calibration, the accuracy was tested by weighing the deposited particles on the sample glass at the atmospheric pressure. The calibration process was repeated for the next time step if it was needed. The mass of deposited asphaltene on the substrate was estimated using the density of extracted asphaltene. Having the total amount of dissolved asphaltene in the space between the glass surface and cell head (volume = glass surface area × height), the weight fraction of deposited asphaltene was calculated. In order to avoid any localized errors, the average amount of deposited asphaltene on nine substrates was reported as the final result. It should be noted that each test session was repeated three times to check the accuracy.

As a side note, based on the microscope imaging, it is possible to focus on the fluid and the solid surface, and therefore the lens was adjusted and focused solely on the glass substrate surface. Thus all dark particles on the images are flocculated asphaltene deposited on the glass surface, not the asphaltene presence in bulk. On the other hand, it is impossible to capture and record the whole asphaltene particles in the bulk of fluid by a microscope because of their different position to the microscope lens. In summary, all the dark particles are the deposited asphaltene on the glass surface.

To evaluate the effects of N_2, CO_2 and CH_4 on the rate of the asphaltene deposition, 10 mol% of the prepared gas was injected into the synthetic oil by a piston-cylinder setup. At the first step, the desired amount of gas was injected into the cylinder, then using an HPLC pump the gas was injected into the high-pressure cell. Steps 1-6 were repeated for CO_2, CH_4, and N_2 injection scenarios.

It is worth mentioning that the minimum miscibility pressure (MMP) was checked theoretically and experimentally for different gas injection scenarios in this study. According to the results, MMP for the mixture of oil and different gases used in this study was less than 30 bar at 90° C. Moreover, in the present research, the amount of deposited asphaltene was investigated at pressures (30, 60, 100 and 140 bar) higher than MMP. Therefore, all the experiments were

conducted under a single-phase condition. In this regard, it could be concluded that whole injected gas can be considered as the solution gas.

The findings of this study may be somewhat limited by; 1) It was impossible to investigate the rate of asphaltene deposition at pressures less than 30 bar because of missing the miscibility condition, 2) The glass surface was used instead of a porous medium to visualize the deposition process.

3. Results and Discussion

3.1. Effects of different gas injection scenarios on asphaltene deposition rate

The images captured at equal time intervals show that the asphaltene particles deposit on the glass surface over time. Image analysis revealed that after approximately 2 hours, the asphaltene deposition process reaches a steady-state condition, meaning that no additional asphaltene deposits are observed on the glass surface after this point.

Fig. 4 clearly shows the impact of pressure increment on the amount of deposited asphaltene. It is worth stressing that dark areas in the images represent flocculated asphaltene deposited on the glass substrates. As can be seen in Fig. 4, pressure increment leads to a higher amount of asphaltene deposition.

Fig. 5 represents the asphaltene deposition at different times for the case without gas injection. The images indicate that the amount of deposited asphaltene increases over time until it reaches the steady state condition. Experimental observations and processing of the images captured after 2 hours revealed that no additional deposition occurs after approximately 2 hours. The images show that as the pressure increases from 30 to 140 bar, the amount of deposited asphaltene increases too. Increasing pressure seems to affect the solubility of asphaltene molecules in solution. For further clarification, the supplementary video shows the movement and asphaltene deposition on the glass substrate at 30 bar and 90˚C.

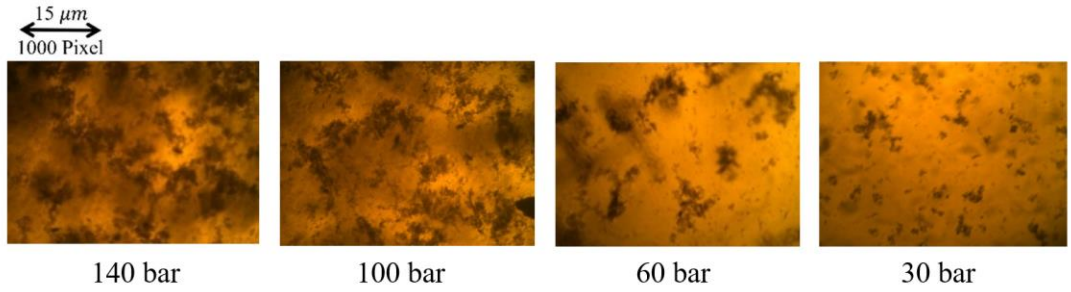

Fig. 4. Effect of pressure on the amount of asphaltene deposition, after 2 hours at 90˚C.

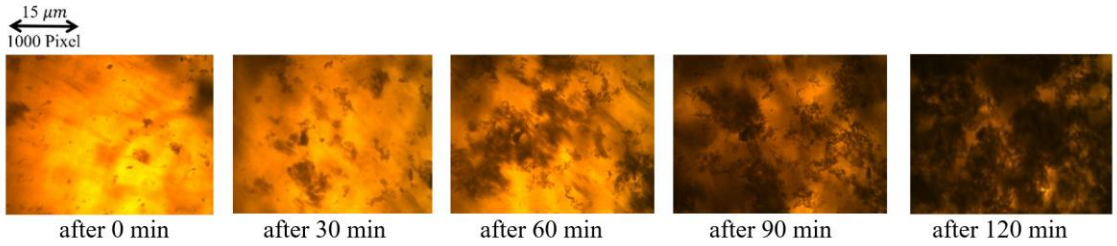

Fig. 5. Asphaltene deposition at different times, without gas injection, 100 bar and 90˚C.

The second part of the current study aims to consider the effect of different gas injection scenarios on the asphaltene deposition process by injecting 10 mol% of CO_2, CH_4 and N_2 into the high-pressure cell using a cylinder-piston setup. Firstly, the specified volume of gas was injected into the cylinder, then using an HPLC pump the gas was injected into the high-pressure cell gradually. The results presented in Figs. 6-8 show a significant difference between the CO_2 injection and without gas injection scenarios. Comparing Figs. 5 and 8 clearly indicate that the injection of CO_2 into the synthetic oil solution results in a higher deposition rate that is up to 1.5 times faster than that observed for the case study without gas injection at 140 bar pressure. Due to the fact that both asphaltene and CO_2 have polar molecules may lead to a higher interaction coefficient between them, finally resulting in higher asphaltene deposition and consequently a faster deposition rate.

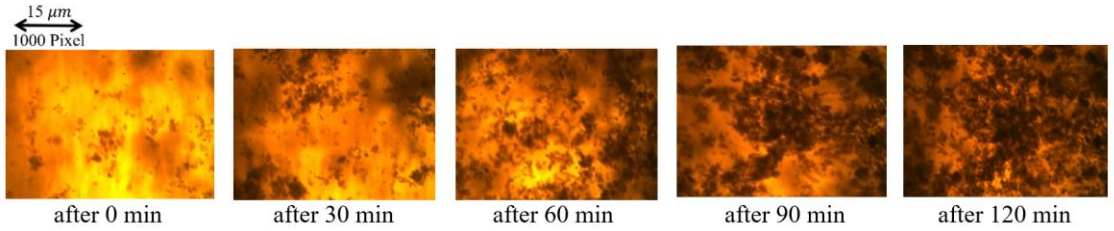

Fig. 6. Asphaltene deposition at various times, 10 mol % N_2 injection, 100 bar and 90˚C.

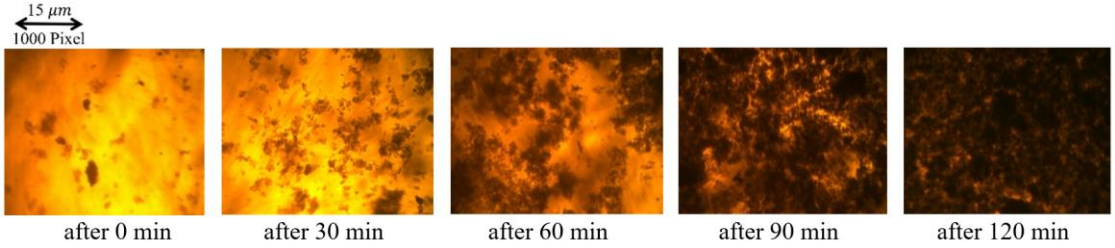

Fig. 7. Asphaltene deposition at different times, 10 mol % CH_4 injection, 100 bar and 90˚C.

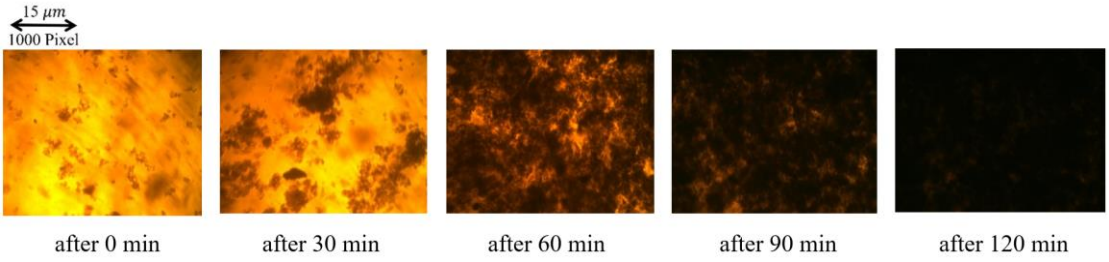

Fig. 8. Asphaltene deposition at different times during 10 mol % CO_2 injection at 100 bar and 90˚C.

Comparing the results presented in Figs. 7 and 8 reveals that the CO_2 injection scenario results in a higher amount of asphaltene deposition comparing the results with CH_4 injection scenario. In order to make a better comparison, Fig. 9 shows the effect of different gas injection scenarios on the amount of asphaltene deposition after 120 min, at 100 bar and 90˚C. It is apparent from the figure that N_2 injection has not a significant impact on the deposition process in contrast to the scenario with injected CO_2 and CH_4. Besides, Fig. 10 compares the effect of different gas injection scenarios on the amount of deposited asphaltene at various pressures which have been evaluated after the steady state condition. These results illustrate both effects of the pressure and different gas injections on the amount of the deposited asphaltene. The quantitative data on deposited

asphaltene versus time at different pressures and different gas injection scenarios are shown in Tables 4-7 for all scenarios.

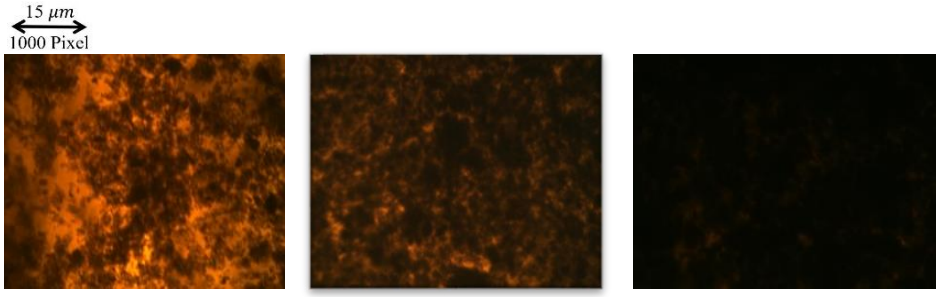

N_2 CH_4 CO_2

Fig. 9. Effects of different gases injection on the asphaltene deposition, after 120 min, at 100 bar and 90˚C.

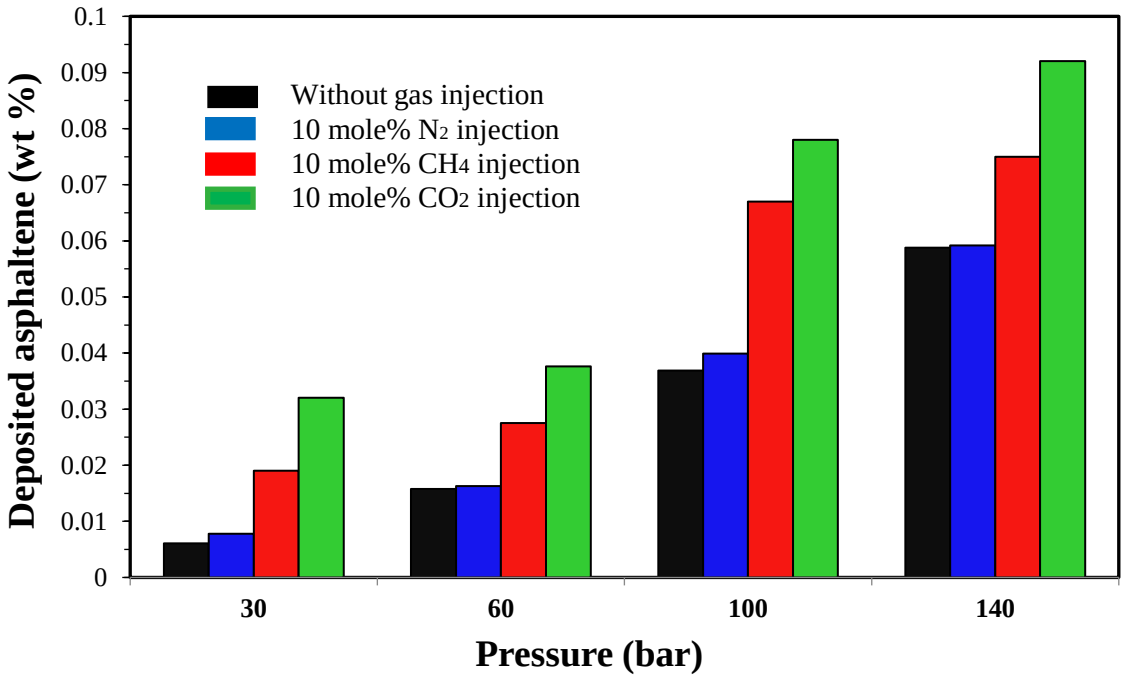

Fig. 10. A comparison of Asphaltene deposition during different gas injection scenarios after 120 min at different pressures and 90˚C.

Table 4.

Asphaltene deposition versus time – without gas injection at 90˚C.

Time (min)	0	30	60	90	120	0	30	60	90	120
Pressure (bar)	Asphaltene deposited (wt %)					Standard deviation				
30	0	0.00100	0.00280	0.00430	0.00610	0	0.00015	0.00040	0.00035	0.00065
60	0	0.00300	0.00800	0.01100	0.01580	0	0.00030	0.00020	0.00250	0.00260
100	0	0.00550	0.01100	0.02690	0.03690	0	0.00095	0.00100	0.00130	0.00180
140	0	0.01000	0.02900	0.04300	0.05880	0	0.00060	0.00350	0.00175	0.00260

Table 5.

Asphaltene deposition versus time – 10 mol % N_2 at 90˚C.

Time (min)	0	30	60	90	120	0	30	60	90	120
Pressure (bar)	Asphaltene deposited (wt %)					Standard deviation				
30	0	0.00120	0.00320	0.00540	0.00780	0	0.00025	0.00045	0.00085	0.00050
60	0	0.00330	0.00890	0.01180	0.01630	0	0.00030	0.00035	0.00105	0.00100
100	0	0.00590	0.01280	0.02880	0.03990	0	0.00040	0.00135	0.00110	0.00080
140	0	0.01100	0.02940	0.04380	0.05920	0	0.00215	0.00195	0.00120	0.00135

Table 6.

Asphaltene deposition versus time – 10 mol % CH_4 at 90˚C.

Time (min)	0	30	60	90	120	0	30	60	90	120
Pressure (bar)	Asphaltene deposited (wt %)					Standard deviation				
30	0	0.00450	0.00830	0.01300	0.01940	0	0.00020	0.00055	0.00105	0.00080
60	0	0.00730	0.01470	0.02100	0.02750	0	0.00025	0.00120	0.00175	0.00135
100	0	0.00930	0.03010	0.05200	0.06700	0	0.00060	0.00215	0.00215	0.00300
140	0	0.01680	0.04900	0.06700	0.07500	0	0.00115	0.00230	0.00250	0.00175

Table 7.

Asphaltene deposition versus time – 10 mol % CO_2 at 90˚C.

Time (min)	0	30	60	90	120	0	30	60	90	120
Pressure (bar)	Asphaltene deposited (wt %)					Standard deviation				
30	0	0.00510	0.01710	0.02140	0.03200	0	0.00040	0.00035	0.00035	0.00055
60	0	0.00870	0.01950	0.02890	0.03760	0	0.00030	0.00075	0.00115	0.00095
100	0	0.01540	0.03660	0.06160	0.07800	0	0.00105	0.00255	0.00110	0.00250
140	0	0.02140	0.05790	0.07120	0.09200	0	0.00155	0.00205	0.00131	0.00320

These results may be explained by the fact that the interaction coefficient between N_2 and asphaltene molecules is less than that between CO_2/CH_4 and asphaltene molecules. Previous research findings on the thermodynamic modelling of asphaltene deposition have confirmed that the interaction coefficient between gas and asphaltene molecules is the critical parameter used to evaluate the amount of asphaltene deposition, where the higher interaction coefficient leads to more asphaltene deposition [22, 70]. Based on the solid model, the interaction coefficient is determined by the following equation [70]:

$$d_{ik} = 1 - \left(\frac{2.\ v_{ci}^{\frac{1}{6}}.v_{ck}^{\frac{1}{6}}}{v_{ci}^{\frac{1}{3}}+v_{ck}^{\frac{1}{3}}}\right)^{e} \qquad \text{i=2,…, 12; k=2,…,12} \qquad (1)$$

where d_{ik} is the interaction coefficient between components i and k, and v_{ci} and v_{ck} are the critical volumes of components i and k, respectively. The interaction coefficients between N_2, CO_2, CH_4 and asphaltene molecules at different mole percent gas injection using the CMG simulator (WinProp fluid property characterization tool) have been compared in Table 8. The higher interaction coefficients between asphaltene molecules and CO_2 and CH_4 confirm our experimental results regarding the higher amount of the asphaltene deposition in these two cases.

Table 8.
The analysis of the interaction coefficient between different gasses and asphaltene molecule [22, 23].

	Gas injection (mol%)			
	0.05	0.10	0.15	0.20
N_2/asphaltene interaction coefficient	0.03	0.04	0.08	0.13
CH_4/asphaltene interaction coefficient	0.10	0.12	0.15	0.22
CO_2/asphaltene interaction coefficient	0.16	0.20	0.24	0.35

To have a better assessment, Figs. 11-14 illustrate asphaltene deposition over time at different operating pressures for different gas injection scenarios. The results indicate that the deposition rate increases notably during CO_2 and CH_4 injection. Also, it could be concluded that CH_4 affects the asphaltene deposition rate more than N_2 and less than CO_2.

It can be seen that the rate of deposition at 140 bar pressure is 10 times faster than at 30 bar pressure. It should be noted that to ensure the accuracy of the results, all of the experimental tests were repeated three times.

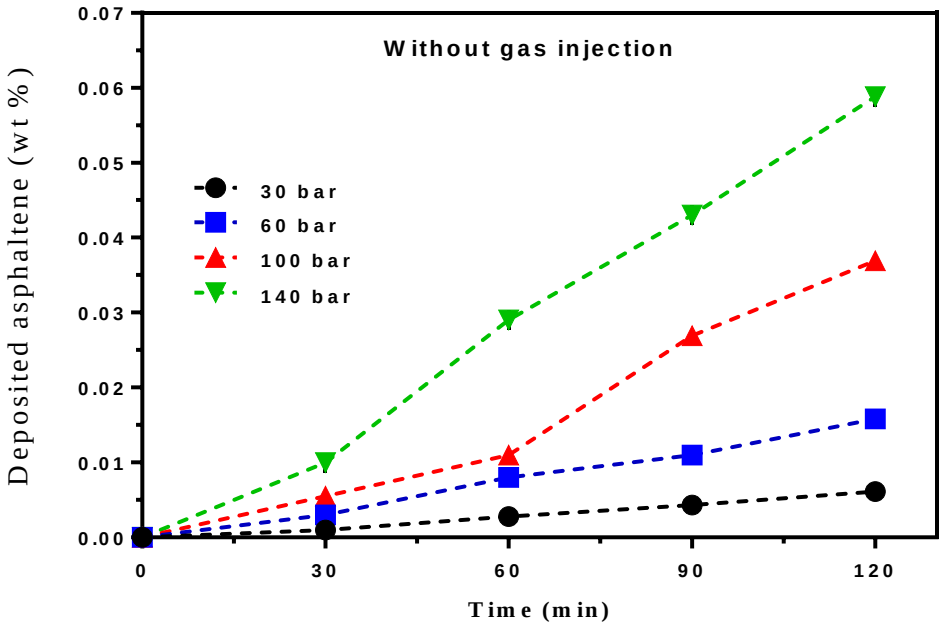

Fig. 11. Asphaltene deposition rate without gas injection at 30, 60, 100 and 140 bar pressures and 90˚C.

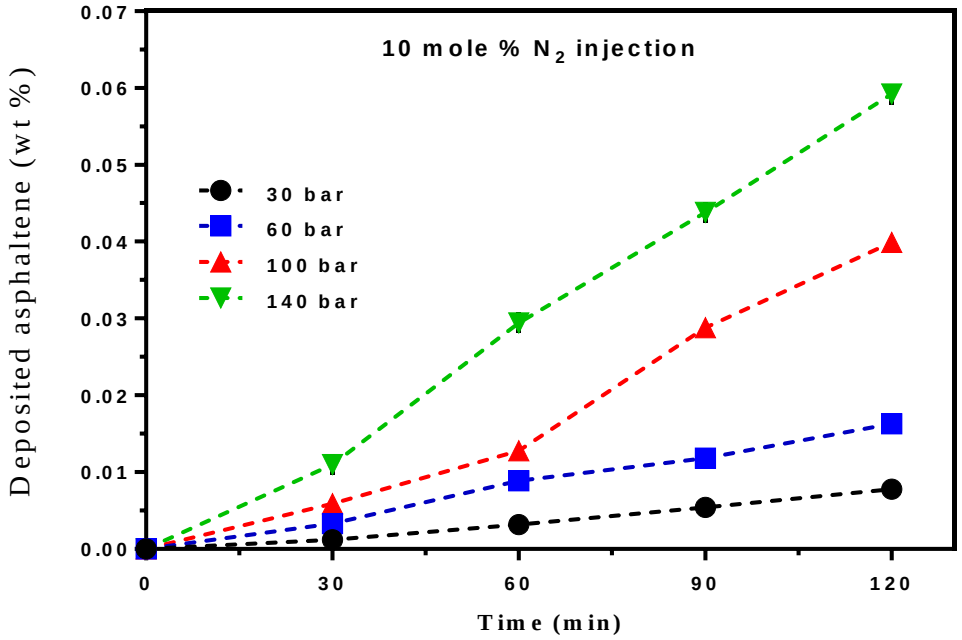

360

361 Fig. 12. Asphaltene deposition rate during 10 mol % N_2 injection at 30, 60, 100 and 140 bar
362 pressures and 90˚C.
363

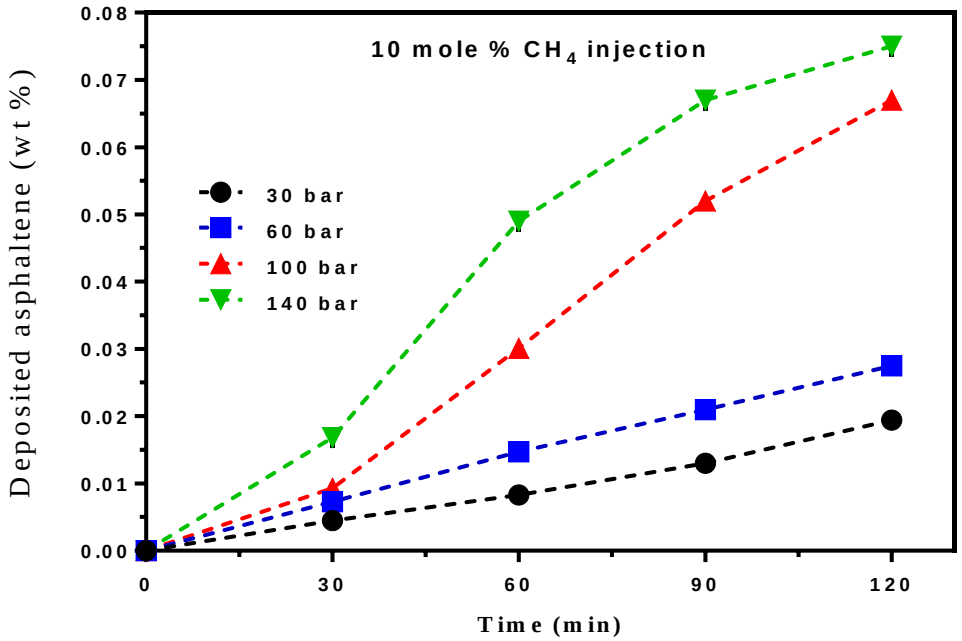

364
365 Fig. 13. Asphaltene deposition rate during 10 mol % CH_4 injection at 30, 60, 100 and 140 bar
366 pressures and 90˚C.
367
368

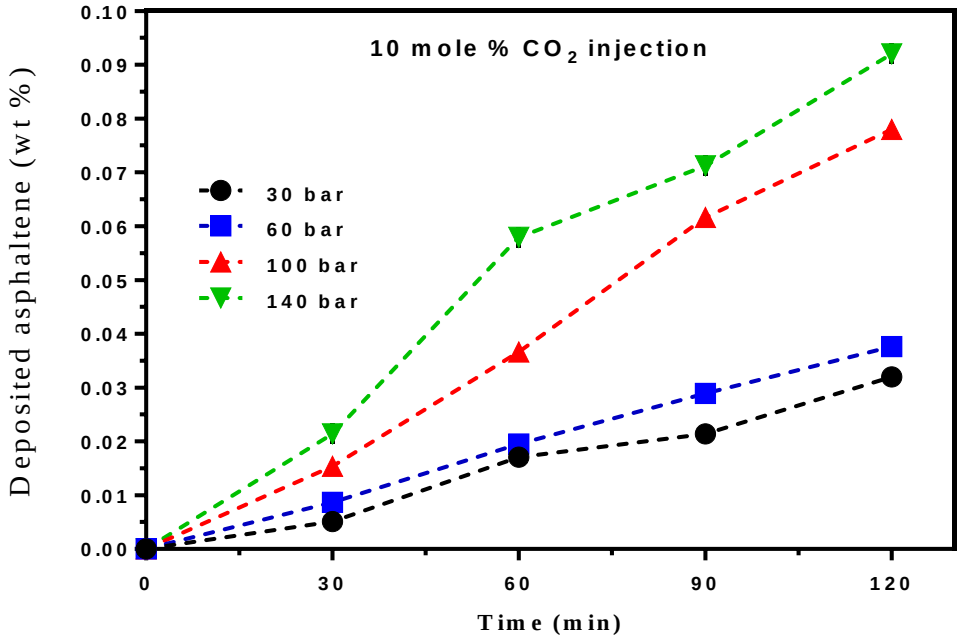

Fig. 14. Asphaltene deposition rate during 10 mol % CO_2 injection at 30, 60, 100 and 140 bar pressures and 90˚C.

3.2. Effects of gas injection on the asphaltene flocculation

Experimental observations showed that gas injection affected asphaltene flocculation and caused asphaltene particles to make bigger flocs [71-73]. Due to the fact that deposition of asphaltene flocs leads to wettability reduction in the porous media of reservoir rocks, this phenomenon could be damaging in gas injection-EOR methods.

In a further analysis in this study, the asphaltene fluctuation behaviour in the presence of the different gas injection scenarios has been examined. Figs. 15-18 show asphaltene flocculation during different gas injection scenarios. To make a better comparison, Fig. 19 shows the effect of gas injection on the size of flocculated asphaltene particles measured by SigmaScan Pro 5^{TM} software. It is apparent from Figs. 15-19 that CH_4 and CO_2 injection leads to the formation of bigger asphaltene flocs compared the results with N_2 injection. However, N_2 injection does not affect asphaltene flocculation significantly. A comparison of results reveals that CO_2 injection influences asphaltene flocculation more than CH_4.

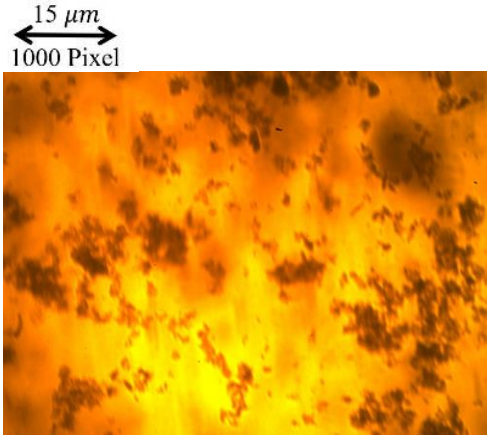

Fig. 15. Asphaltene flocculation without gas injection at 140 bar and 90°C.

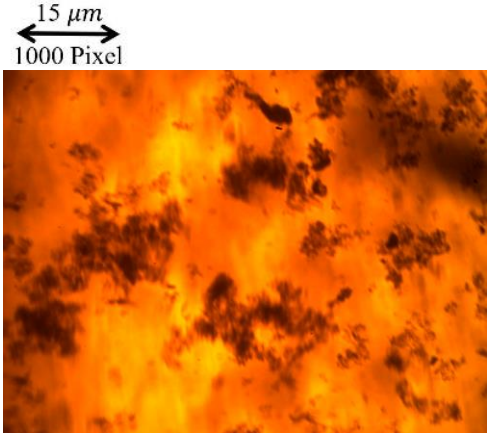

Fig. 16. Asphaltene flocculation with 10 mole% N_2 injection at 140 bar and 90°C.

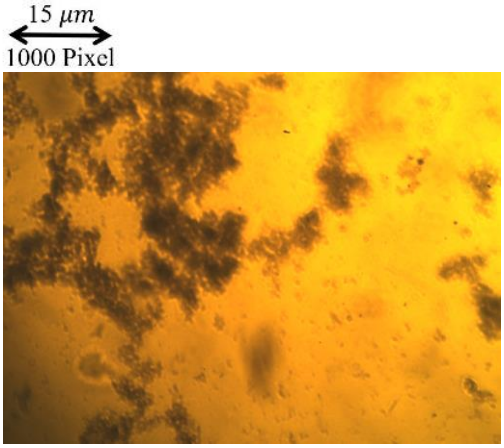

Fig. 17. Asphaltene flocculation with 10 mole% CH_4 injection at 140 bar and 90°C.

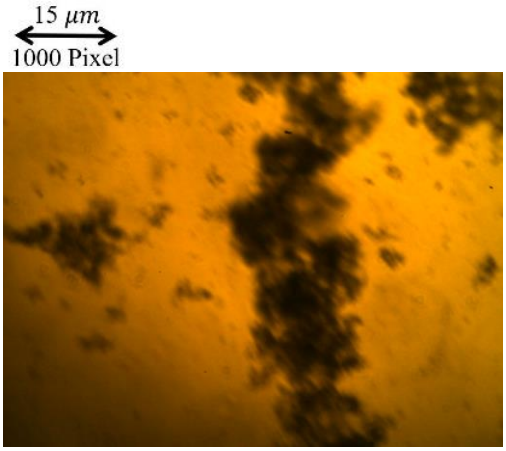

Fig. 18. Asphaltene flocculation with 10 mole% CO_2 injection at 140 bar and 90°C.

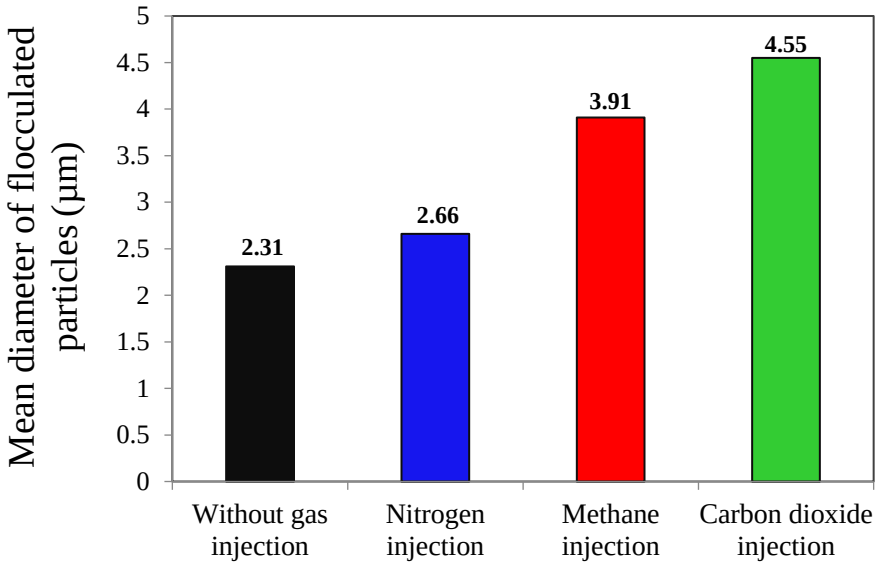

Fig. 19. Effects of different gas injection scenarios on asphaltene flocculation at 140 bar and 90°C.

4. Conclusions

Asphaltene deposition during EOR processes is of particular concern in the oil industry. A proper understanding of the asphaltene deposition mechanism would help researchers to develop methods for asphaltene inhibition or treatment. The present study was designed to determine the effect of different gas injection processes as EOR methods on the asphaltene deposition rate at different pressure conditions. A series of experiments were conducted in a high-pressure cell to investigate the deposition rate under various gas injection scenarios. The following major findings are identified in the current paper:

- According to the results, when there is no gas injection, the rate of asphaltene deposition increases as the pressure increases. For example, the rate of deposition at 140 bar is 11.7 times greater than that at 30 bar pressure.
- The results obtained with different gas injection scenarios revealed that CO_2 and CH_4 affect the rate of deposition and lead to a significant increase in the amount of deposition. For instance, at 140 bar and 90˚C, the amount of deposited asphaltene without gas injection is 0.05880 wt %, increasing to 0.07500 and 0.09200 wt% for 10 mol% injection of CH_4 and

CO_2, respectively. Taken together, the results suggest that carbon dioxide results in more deposition than methane and N_2 at the same gas injection concentration.

- Based on the experimental results, N_2 injection had a minimum effect on the rate of deposition compared with CH_4 and CO_2 injection scenarios.
- The effect of gas injection on asphaltene flocculation was investigated. It was revealed that gas injection affects the flocculation process. The results showed that CO_2 and CH_4 injection leads to the formation of bigger asphaltene flocs in comparison with N_2. However, N_2 injection did not affect asphaltene flocculation significantly. The results of this study provide valuable insights into the mechanism asphaltene deposition rate due to the different gas injection scenarios.

References

[1] D.L. Mitchell, J.G. Speight, The solubility of asphaltenes in hydrocarbon solvents, Fuel, 52 (1973) 149-152.

[2] J.G. Speight, The Chemistry and Technology of Petroleum, Fifth ed., Taylor & Francis, 2014.

[3] H. Groenzin, O.C. Mullins, Molecular size and structure of asphaltenes from various sources, Energy & Fuels, 14 (2000) 677-684.

[4] A.R. Hortal, B. Martínez-Haya, M.D. Lobato, J.M. Pedrosa, S. Lago, On the determination of molecular weight distributions of asphaltenes and their aggregates in laser desorption ionization experiments, Journal of Mass Spectrometry, 41 (2006) 960-968.

[5] G.C. Klein, S. Kim, R.P. Rodgers, A.G. Marshall, A. Yen, S. Asomaning, Mass spectral analysis of asphaltenes. I. Compositional differences between pressure-drop and solvent-drop asphaltenes determined by electrospray ionization fourier transform ion cyclotron resonance mass spectrometry, Energy & Fuels, 20 (2006) 1965-1972.

[6] G.A. Mansoori, D. Vazquez, M. Shariaty-Niassar, Polydispersity of heavy organics in crude oils and their role in oil well fouling, Journal of Petroleum Science and Engineering, 58 (2007) 375-390.

[7] G.A. Mansoori, Modeling of asphaltene and other heavy organic depositions, Journal of Petroleum Science and Engineering, 17 (1997) 101-111.

[8] J.G. Speight, Structure of petroleum asphaltenes - Current concepts, in: Alberta Res Counc Inf Ser, 1978.

[9] B. Azinfar, A. Haddadnia, M. Zirrahi, H. Hassanzadeh, J. Abedi, Effect of Asphaltene on Phase Behavior and Thermophysical Properties of Solvent/Bitumen Systems, Journal of Chemical & Engineering Data, 62 (2017) 547-557.

[10] D. Eskin, O. Mohammadzadeh, K. Akbarzadeh, S. Taylor, J. Ratulowski, Reservoir impairment by asphaltenes: A critical review, The Canadian Journal of Chemical Engineering, 94 (2016) 1202-1217.

[11] S.P. Tan, X. Qiu, M. Dejam, H. Adidharma, Critical Point of Fluid Confined in Nanopores: Experimental Detection and Measurement, The Journal of Physical Chemistry C, 123 (2019) 9824-9830.

[12] X. Qiu, S.P. Tan, M. Dejam, H. Adidharma, Simple and accurate isochoric differential scanning calorimetry measurements: phase transitions for pure fluids and mixtures in nanopores, Physical Chemistry Chemical Physics, 21 (2019) 224-231.
[13] X. Qiu, S.P. Tan, M. Dejam, H. Adidharma, Novel isochoric measurement of the onset of vapor–liquid phase transition using differential scanning calorimetry, Physical Chemistry Chemical Physics, 20 (2018) 26241-26248.
[14] J.H. Pacheco-Sanchez, G.A. Mansoori, Prediction of the phase behavior of asphaltene micelle/aromatic hydrocarbon systems, Petroleum Science and Technology, 16 (1998) 377-394.
[15] W. Chaisoontornyotin, A.W. Bingham, M.P. Hoepfner, Reversibility of Asphaltene Precipitation Using Temperature-Induced Aggregation, Energy & Fuels, 31 (2017) 3392-3398.
[16] M.P. Hoepfner, V. Limsakoune, V. Chuenmeechao, T. Maqbool, H.S. Fogler, A Fundamental Study of Asphaltene Deposition, Energy & Fuels, 27 (2013) 725-735.
[17] S.J. Park, G.A. Mansoori, Aggregation and deposition of heavy organics in petroleum crudes, Energy Sources, 10 (1988) 109-125.
[18] K.J. Leontaritis, G.A. Mansoori, Asphaltene deposition: a survey of field experiences and research approaches, Journal of Petroleum Science and Engineering, 1 (1988) 229-239.
[19] F. Soorghali, A. Zolghadr, S. Ayatollahi, Effect of resins on asphaltene deposition and the changes of surface properties at different pressures: A microstructure study, Energy & Fuels, 28 (2014) 2415-2421.
[20] S.I. Andersen, Effect of precipitation temperature on the composition of N-Heptane asphaltenes Part 2, Fuel Science and Technology International, 13 (1995) 579-604.
[21] P. Zanganeh, S. Ayatollahi, A. Alamdari, A. Zolghadr, H. Dashti, S. Kord, Asphaltene Deposition during CO_2 Injection and Pressure Depletion: A Visual Study, Energy & Fuels, 26 (2012) 1412-1419.
[22] P. Zanganeh, H. Dashti, S. Ayatollahi, Visual investigation and modeling of asphaltene precipitation and deposition during CO_2 miscible injection into oil reservoirs, Fuel, 160 (2015) 132-139.
[23] P. Zanganeh, H. Dashti, S. Ayatollahi, Comparing the effects of CH_4, CO_2, and N_2 injection on asphaltene precipitation and deposition at reservoir condition: A visual and modeling study, Fuel, 217 (2018) 633-641.
[24] J.L. Creek, Freedom of action in the state of asphaltenes: Escape from conventional wisdom, Energy & Fuels, 19 (2005) 1212-1224.
[25] A. Mirvakili, M.R. Rahimpour, A. Jahanmiri, Effect of a cationic surfactant as a chemical destabilization of crude oil based emulsions and asphaltene stabilized, Journal of Chemical & Engineering Data, 57 (2012) 1689-1699.
[26] A. Yen, Y.R. Yin, S. Asomaning, Evaluating Asphaltene Inhibitors: Laboratory Tests and Field Studies, in: SPE International Symposium on Oilfield Chemistry, Society of Petroleum Engineers, Houston, Texas, 2001, pp. 7.
[27] L.M. Cenegy, Survey Of Successful World-wide Asphaltene Inhibitor Treatments In Oil Production Fields, in: SPE Annual Technical Conference and Exhibition, Society of Petroleum Engineers, New Orleans, Louisiana, 2001, pp. 7.
[28] M. Alhreez, D. Wen, Controlled releases of asphaltene inhibitors by nanoemulsions, Fuel, 234 (2018) 538-548.
[29] L.C. Rocha Junior, M.S. Ferreira, A.C. da Silva Ramos, Inhibition of asphaltene precipitation in Brazilian crude oils using new oil soluble amphiphiles, Journal of Petroleum Science and Engineering, 51 (2006) 26-36.

[30] A.A. Cruz, M. Amaral, D. Santos, A. Palma, E. Franceschi, G.R. Borges, J.A.P. Coutinho, J. Palácio, C. Dariva, CO2 influence on asphaltene precipitation, The Journal of Supercritical Fluids, 143 (2019) 24-31.
[31] R.O. Idem, H.H. Ibrahim, Kinetics of CO_2-induced asphaltene precipitation from various Saskatchewan crude oils during CO_2 miscible flooding, Journal of Petroleum Science and Engineering, 35 (2002) 233-246.
[32] S. Kord, H. Dashti, P. Zanganeh, S. Ayatollahi, Evaluation of the kinetics of asphaltene flocculation during natural depletion and CO_2 injection in heptane-toluene mixtures, in, Society of Petroleum Engineers, 2017.
[33] L.W. Lake, Fundamentals of Enhanced Oil Recovery, SPE, 1986.
[34] V. Alvarado, E. Manrique, Enhanced Oil Recovery: Field Planning and Development Strategies, Elsevier Science, 2010.
[35] S.O. Olayiwola, M. Dejam, A comprehensive review on interaction of nanoparticles with low salinity water and surfactant for enhanced oil recovery in sandstone and carbonate reservoirs, Fuel, 241 (2019) 1045-1057.
[36] P. Rostami, M.F. Mehraban, M. Sharifi, M. Dejam, S. Ayatollahi, Effect of water salinity on oil/brine interfacial behaviour during low salinity waterflooding: A mechanistic study, Petroleum, (2019).
[37] V. Mashayekhizadeh, S. Kord, M. Dejam, EOR Potential within Iran, Special Topics & Reviews in Porous Media: An International Journal, 5 (2014) 325-354.
[38] A. Al-Adasani, B. Bai, Recent developments and updated screening criteria of enhanced oil recovery techniques, in, Society of Petroleum Engineers, 2010.
[39] S.H. Talebian, R. Masoudi, I.M. Tan, P.L.J. Zitha, Foam assisted CO_2-EOR: A review of concept, challenges, and future prospects, Journal of Petroleum Science and Engineering, 120 (2014) 202-215.
[40] B. Jia, J.-S. Tsau, R. Barati, A review of the current progress of CO2 injection EOR and carbon storage in shale oil reservoirs, Fuel, 236 (2019) 404-427.
[41] S.O. Olayiwola, M. Dejam, Mathematical modelling of surface tension of nanoparticles in electrolyte solutions, Chemical Engineering Science, 197 (2019) 345-356.
[42] E. Amirian, M. Dejam, Z. Chen, Performance forecasting for polymer flooding in heavy oil reservoirs, Fuel, 216 (2018) 83-100.
[43] H. Saboorian-Jooybari, M. Dejam, Z. Chen, Heavy oil polymer flooding from laboratory core floods to pilot tests and field applications: Half-century studies, Journal of Petroleum Science and Engineering, 142 (2016) 85-100.
[44] H. Saboorian-Jooybari, M. Dejam, Z. Chen, Half-Century of Heavy Oil Polymer Flooding from Laboratory Core Floods to Pilot Tests and Field Applications, in: SPE Canada Heavy Oil Technical Conference, Society of Petroleum Engineers, Calgary, Alberta, Canada, 2015, pp. 26.
[45] H. Dashti, P. Zanganeh, S. Ayatollahi, The Comparison between Heavy and Light Oil Asphaltene Deposition during Pressure Depletion and CO_2 Injection at Reservoir Condition, A Visual Laboratory Study, in: Chemeca 2013 - Brisbane, Engineers Australia, 2013.
[46] M. Cao, Y. Gu, Oil recovery mechanisms and asphaltene precipitation phenomenon in immiscible and miscible CO_2 flooding processes, Fuel, 109 (2013) 157-166.
[47] T. Jafari Behbahani, C. Ghotbi, V. Taghikhani, A. Shahrabadi, Investigation of asphaltene adsorption in sandstone core sample during CO_2 injection: Experimental and modified modeling, Fuel, 133 (2014) 63-72.

[48] S. Kord, O. Mohammadzadeh, R. Miri, B.S. Soulgani, Further investigation into the mechanisms of asphaltene deposition and permeability impairment in porous media using a modified analytical model, Fuel, 117, Part A (2014) 259-268.
[49] D.L. Gonzalez, E. Mahmoodaghdam, F.H. Lim, N.B. Joshi, Effects of gas additions to deepwater Gulf of Mexico reservoir oil: Experimental investigation of asphaltene precipitation and deposition, in, Society of Petroleum Engineers, 2012.
[50] A.K.M. Jamaluddin, N. Joshi, F. Iwere, O. Gurpinar, An investigation of asphaltene instability under Nitrogen injection, in, Society of Petroleum Engineers, 2002.
[51] Y. Kazemzadeh, R. Parsaei, M. Riazi, Experimental study of asphaltene precipitation prediction during gas injection to oil reservoirs by interfacial tension measurement, Colloids and Surfaces A: Physicochemical and Engineering Aspects, 466 (2015) 138-146.
[52] S. Moradi, M. Dabiri, B. Dabir, D. Rashtchian, M.A. Emadi, Investigation of asphaltene precipitation in miscible gas injection processes: experimental study and modeling, Brazilian Journal of Chemical Engineering, 29 (2012) 665-676.
[53] S. Negahban, J.N.M. Bahamaish, N. Joshi, J. Nighswander, A.K.M. Jamaluddin, An experimental study at an Abu Dhabi reservoir of asphaltene precipitation caused by gas injection, (2005).
[54] N. Arsalan, S.S. Palayangoda, Q.P. Nguyen, Characterization of asphaltene deposition in a stainless steel tube, Journal of Petroleum Science and Engineering, 121 (2014) 66-77.
[55] T. Maqbool, A.T. Balgoa, H.S. Fogler, Revisiting asphaltene precipitation from crude oils: A case of neglected kinetic effects, Energy & Fuels, 23 (2009) 3681-3686.
[56] T. Maqbool, S. Raha, M.P. Hoepfner, H.S. Fogler, Modeling the aggregation of asphaltene nanoaggregates in crude oil−precipitant systems, Energy & Fuels, 25 (2011) 1585-1596.
[57] C.W. Angle, Y. Long, H. Hamza, L. Lue, Precipitation of asphaltenes from solvent-diluted heavy oil and thermodynamic properties of solvent-diluted heavy oil solutions, Fuel, 85 (2006) 492-506.
[58] R. Moghadasi, S. Kord, J. Moghadasi, H. Dashti, Mechanistic understanding of asphaltenes surface behavior at oil/water interface: An experimental study, Journal of Molecular Liquids, 285 (2019) 562-571.
[59] M. Jamialahmadi, B. Soltani, H. Müller-Steinhagen, D. Rashtchian, Measurement and prediction of the rate of deposition of flocculated asphaltene particles from oil, International Journal of Heat and Mass Transfer, 52 (2009) 4624-4634.
[60] B.S. Soulgani, B. Tohidi, M. Jamialahmadi, D. Rashtchian, Modeling formation damage due to asphaltene deposition in the porous media, Energy & Fuels, 25 (2011) 753-761.
[61] F. Salimi, M.V. Seftie, S. Ayatollahi, Experimental investigation of the effects of different parameters on the rate of asphaltene deposition in laminar flow and its prediction using heat transfer approach, Journal of Dispersion Science and Technology, 34 (2013) 1690-1696.
[62] M. Haghshenasfard, K. Hooman, CFD modeling of asphaltene deposition rate from crude oil, Journal of Petroleum Science and Engineering, 128 (2015) 24-32.
[63] V.B.C. Fávero, A. Hanpan, P. Phichphimok, K. Binabdullah, H.S. Fogler, Mechanistic investigation of asphaltene deposition, Energy & Fuels, (2016).
[64] A.K. Ghahfarokhi, P. Kor, R. Kharrat, B.S. Soulgani, Characterization of asphaltene deposition process in flow loop apparatus; An experimental investigation and modeling approach, Journal of Petroleum Science and Engineering, 151 (2017) 330-340.

[65] J. Sayyad Amin, A. Alamdari, N. Mehranbod, S. Ayatollahi, E. Nikooee, Prediction of asphaltene precipitation: Learning from data at different conditions, Energy & Fuels, 24 (2010) 4046-4053.
[66] J. Sayyad Amin, S. Ayatollahi, A. Alamdari, Fractal characteristics of an asphaltene deposited heterogeneous surface, Applied Surface Science, 256 (2009) 67-75.
[67] A.S.f.T.a. Materials, Annual Book of ASTM Standard, Philadelphia, PA, 2005.
[68] J.S. Amin, E.Nikooee, M.H. Ghatee, S. Ayatollahi, A. Alamdari, T. Sedghamiz, Investigating the effect of different asphaltene structures on surface topography and wettability alteration, Applied Surface Science, 257 (2011) 8341-8349.
[69] H. Dashti, S. Kord, A. Shariati, S. Ayatollahi, M. Moshfeghian, P. Zanganeh, Thermodynamic Fluid Characterization of an Iranian Oil Reservoir, in: Near Surface 2011-17th EAGE European Meeting of Environmental and Engineering Geophysics, Leicester, United Kingdom, 2011.
[70] L.X. Nghiem, B.F. Kohse, P.H. Sammon, Compositional simulation of the vapex process, in, Petroleum Society of Canada, 2000.
[71] K. Rastegari, W.Y. Svrcek, H.W. Yarranton, Kinetics of Asphaltene Flocculation, Industrial & Engineering Chemistry Research, 43 (2004) 6861-6870.
[72] V.A.M. Branco, G.A. Mansoori, L.C. De Almeida Xavier, S.J. Park, H. Manafi, Asphaltene flocculation and collapse from petroleum fluids, Journal of Petroleum Science and Engineering, 32 (2001) 217-230.
[73] J.A. Duran, Y.A. Casas, L. Xiang, L. Zhang, H. Zeng, H.W. Yarranton, Nature of Asphaltene Aggregates, Energy & Fuels, (2018).